Performance Assessment of the BLDC Motor in EV Drives using Nonlinear Model Predictive Control

Pramod Ubare
Department of Instrumentation and Control
College of Engineering Pune
Maharashtra, India
upr18.instru@coep.ac.in

D. N. Sonawane
Department of Instrumentation and Control
College of Engineering Pune
Maharashtra, India
dns.instru@coep.ac.in

Received: 11 April 2022 | Revised: 28 April 2022 | Accepted: 8 May 2022

Abstract-In this paper, the Nonlinear Model Predictive Control (NMPC) technique is proposed for the control of BrushLess Direct Current (BLDC) motors to address the problem of over-excitation, specifically in Electric Vehicle (EV) applications. This over-excitation increases the overall energy consumption of the machine and eventually reduces the vehicle's driving range. The developed NMPC incorporates a nonlinear model of the BLDC motor with EV load and obtains the optimal current through the optimal voltage applied to the machine to regulate the motor torque. The proposed NMPC is compared with three conventional control techniques, the Field-Oriented Control (FOC), the Direct Torque Control (DTC), and the hybrid (the combination of DTC and FOC) control. It is observed from the simulation results that the proposed NMPC controller is more energy efficient while maintaining performance. This paper also discusses the selection of the motor based on the specified vehicle requirements. This has been done by matching the vehicle speed-torque characteristic curve with the motor's one.

Keywords-BLDC motor; model predictive control; nonlinear systems; optimization; electric vehicle

I. INTRODUCTION

Electric vehicles (EVs) are a zero-emission solution for vehicular technology. They are the attractive alternative to the traditional Internal Combustion (IC) engines [1]. The, technology advancement in EV and energy management solutions are the top priority areas of the relative research. Traction motor, the main component of the power-train, consumes the most power from the batteries [1]. Several types of electric motors are used for the traction in EVs, such as Induction Motors (IMs), Permanent Magnet Motors (PMMs), Switched Reluctance Motors (SRMs), etc. In this work, a Brushless Direct Current (BLDC) motor, which is a type of PMM [2, 3], is considered. The driving range can be improved by the optimal usage of the available energy for the traction system. The application of control system engineering to control the BLDC motor has gained significant attention by ensuring the efficient and reliable operation of the motor [2-4]. Conventional control techniques have been utilized in the speed/torque control of BLDC motor for various applications. Its combination with fuzzy logic improves performance [5, 6].

The FOC is a vector control technique proposed mainly for the control of AC synchronous and IMs [7]. However, features like ripple reduction and better efficiency have been used in the BLDC motor control [8-10]. Due to these advantages, authors in [11, 12] tried the FOC principle to find the optimal current excitation component as an extension over the main controller. Another widely accepted control technique for the AC motors is the DTC [13, 14]. It has been primarily proposed for IMs and has been then utilized in BLDC motor control [15, 16]. In the DTC technique, the control actions (stator voltages and currents) are obtained from a switching table implemented with a Look-Up-Table (LUT). FOC and DTC have their own advantages and disadvantages. Recently, authors in [4] demonstrated the advantages of hybrid control (a combination of DTC and FOC) for the BLDC motor control in aerial drones. The experimental results show that the hybrid controller reduces the speed ripple in the steady state region compared to DTC and decreases the response time compared to FOC. Generalized Predictive Control (GPC) for a BLDC motor is presented in [17]. In GPC, the objective function needs to be computed for all possible switching states, which increases the controller's computational complexity [12, 18].

In this paper, the use of NMPC technique for the torque control with the BLDC prediction model is proposed. The objective function comprises of: (1) torque reference tracking, (2) current d-component minimization, which avoids the over-actuation of the motor, and (3) input regulation to minimize the required voltage in order to achieve the desired torque, while it also works as an integrator to reduce steady-state errors. Applicability of the NMPC in the BLDC motor control has been less addressed in the literature, but it has been successfully applied to Permanent Magnet Synchronous Motors (PMSMs) [11], where motor current excitation is always sinusoidal. In this paper, we improved the BLDC motor control performance using NMPC in various directions. The result was compared with 3 control techniques considering various key performance indices. All the control methods were validated through their speed-torque characteristics against the ideal characteristic of the EV, which is generated through the vehicle's effective weight, required acceleration, maximum grading, and speed range. All techniques were realized in

Corresponding author: Pramod Ubare

Matlab, and the proposed NMPC was realized in the CasADi [19] platform with a Matlab interface.

II. MODELING OF SYSTEM DYNAMICS

This section presents the nonlinear mathematical model of the BLDC motor and the EV coupled with the BLDC motor model.

A. BLDC Motor Model

The electrically modeled 3-phase BLDC motor is shown in Figure 1. For simplicity reasons, self and mutual inductance were considered constant. The mathematical model for the BLDC motor is expressed as:

$$v_a = Ri_a + L\frac{di_a}{dt} + E_a \quad (1)$$

where v_a is the phase voltage (V), i_a is the phase current (A), E_a, E_b, and E_c are the back-EMF phase in (V), R is the resistance per phase (Ω), L is the inductance per phase (H). Similar equations can be produce by replacing the suffix *a* with *b* and *c* to get the electrical equations of the other phases. This motor is supplied with 3 phase voltages which are in 120^0 phase shift from each other. The mechanical dynamics for the motor are:

$$T_e = k_f\omega_m + J\frac{d\omega_m}{dt} + T_L \quad (2)$$

where T_e is the generated electrical torque to handle motor load (Nm), T_L is the mechanical load on the motor (Nm), J is rotor's inertia (kgm^2), k_f is the frictional constant (Nm/rad), and ω_m is the rotor speed (rad/sec). The BEMF in the stator is a function of rotor position (electrical angle θ_e) and it is trapezoidal in nature:

$$F(\theta_e) = \begin{cases} 1, & 0 \le \theta_e \le \frac{2\Pi}{3} \\ 1 - \frac{1}{\Pi}(\theta_e - \frac{2\Pi}{3}), & \frac{2\Pi}{3} \le \theta_e \le \Pi \\ -1, & \Pi \le \theta_e \le \frac{5\Pi}{3} \\ -1 + \frac{6}{\Pi}(\theta_e - \frac{5\Pi}{3}), & \frac{5\Pi}{3} \le \theta_e \le 2\Pi \end{cases} \quad (3)$$

The phase-wise BEMF and the electric torque generated are given by:

$$E = \frac{k_e}{2}\omega_m F(\theta_e) \quad (4a)$$

$$T_e = \frac{k_t}{2}\left[F(\theta_e)i_a + F(\theta_e - \frac{2\Pi}{3})i_b + F(\theta_e + \frac{2\Pi}{3})i_c\right] \quad (4b)$$

B. D-Q Modeling of the Motor

The control aspect abc frame of reference is not suitable, as in the abc frame of reference, the motor voltage and current are oscillatory, even under constant speed and load. This makes it unsuitable to use in control law formulation. In the D-Q frame of reference, the voltage and currents are constant for constant speed and torque. Therefore, using Clerk and Park transformation, the abc frame of reference will be converted into the D-Q frame of reference. In the D-Q domain the equations become:

$$v_d = Ri_d + L\frac{di_d}{dt} + \omega_r Li_q + E_d \quad (5a)$$

$$v_q = Ri_q + L\frac{di_q}{dt} + \omega_r Li_d + E_q \quad (5b)$$

where E_d, E_q are the BEMF functions of the electrical angle theta generated from the (4a).

C. Vehicle Model

All the effective forces are taken into account. Figure 1 represents the schematic of these forces [20], which are: the aerodynamic drag (F_w), the acceleration resistance (F_a), the rolling resistance (F_r), and the uphill resistance (F_g). The tractive force (F_t) required to drive the car is cumulative of all the above-mentioned forces [20]. It is represented as:

$$F_t = F_r + F_w + F_g + F_a \quad (6)$$

Substituting the respective equations for all forces we have:

$$F_t = \mu_{rr}Mg\cos(\theta) + Mg\sin(\theta) + \frac{1}{2}\rho A_f C_d V_s^2 + \lambda M\frac{dV_s}{dt} \quad (7)$$

where λ is the rotational inertia constant and V_a is the vehicle velocity (m/sec). The details of the other variables are given in Table II.

The total tractive force F_t is nothing but the mechanical load on the motor in the form of linear force (N). The load torque applied to the BLDC motor is:

$$T_L = F_t\frac{r_w}{G} \quad (8)$$

where r_w is vehicle's wheel radius (m) and G is the gear ratio.

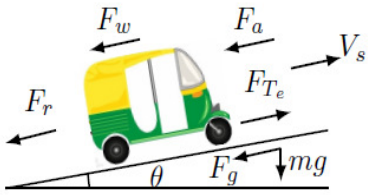

Fig. 1. Schematic of the vehicle showing the tractive forces acting on it.

The EV and BLDC motors are coupled, this modifies the torque equation (2), which becomes [21]:

$$T_e = k_f\omega_m + (J + M(\frac{r_w}{G})^2)\frac{d\omega_m}{dt} + \frac{r_w}{G}(F_r + F_w + F_g) \quad (9)$$

D. Motor Sizing and Driving Cycle

The vehicle requirements specified in Table I were considered to obtain the motor torque requirement. The vehicle parameters given in Table II are taken from [20].

TABLE I. THREE WHEELER EV OPERATING PARAMETERS

Parameter	Value	Unit
Maximum speed	50	Km/h
Maximum acceleration	2	m/s^2
Maximum grading	10	%

Using the vehicle model from Section II, we can get the different characteristic curves of the vehicle, by substituting the values for acceleration, speed, grading (road angle), etc. The speed-torque characteristic specified vehicle is generated and presented in Figure 3. T1 is the minimum torque required to maintain the respective speed, T2 is the minimum torque required to get an acceleration of $2m/s^2$ for the respective speed, T3 is the minimum torque required to maintain the respective speed under 10% grading, and P1, P2, P3, P4 are constant power profiles of 1, 2, 3, and 4KW respectively. Out of these lines, the 3KW line fulfills the requirement with maximum speed of 60Kmph and can maintain constant speed of 26Kmph on maximum grading of 10%. Therefore, the 3KW motor is appropriate for the three-wheeler EV. Its specifications are given in Table II [21].

TABLE II. EV SPECIFICATIONS [21]

Parameter	Notation	Value	Unit
Mass	M	600	kg
Gravitational constant	g	9.81	m/s^2
Air density	ρ	1.225	Kg/m^3
Drag coefficient	C_d	0.5	-
Area	A_f	2.09	m^2
Rolling resistance coefficient	μ_{rr}	0.0015	-
Gear ratio	G	5	-
Wheel radius	r_W	0.19	m
Road angle	θ	1	rad

Taking reference from Figure 2, the torque and speed values are noted in Table III. This derives the gear ratio of 10 to match the vehicle and motor's torque and speed.

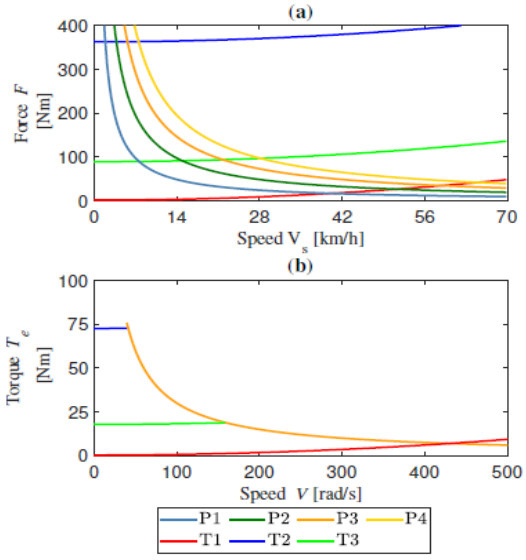

Fig. 2. Vehicle torque-speed characteristic curves. (a) vehicle characteristics with constant power profiles and constant acceleration lines, (b) minimum torque required for the desired speed with the 3KW powered vehicle.

TABLE III. GEAR RATIO DESIGN BASED ON VEHICLE REQUIREMENTS AND MOTOR SPECIFICATIONS

Object	Torque (Nm)	Speed (r/s)
Vehicle (maximum required)	378	81
Motor (rated)	80	367
Gear ratio	1:5	

Figure 3(b) shows the minimum requirements of speed and torque to match the vehicle requirements. The speed-torque curve of the controller should be above the shown curve in Figure 3(b).

III. CONTROL TECHNIQUES

This section presents the design and implementation of 4 control techniques (DTC, FOC, hybrid, and NMPC) under consideration for the assessment of BLDC motor with EV as the load.

A. Field Oriented Control

The fundamental idea behind the FOC technique is making torque and flux components distinct and then control them independently. The block diagram of FOC for the BLDC motor control is shown in Figure 3.

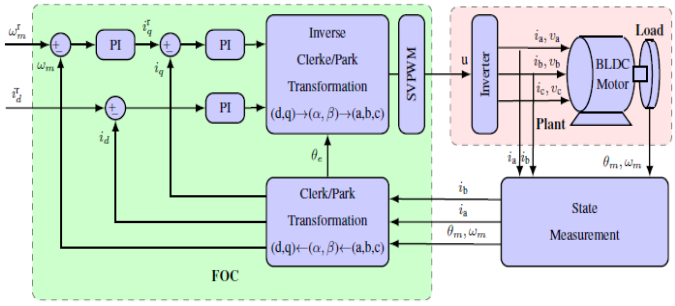

Fig. 3. Block diagram of the BLDC motor control in FOC technique.

Even though this method efficiently controls the machine, it is a parameter-dependent method, for example, the stator or rotor resistances are affected by temperature. Therefore, the FOC is not robust to parameter variations.

B. Direct Torque Control

DTC allows direct controls of the electromagnetic torque and stator flux through a suitable combination of control signals applied to inverter switches. As it directly controls the inverter switches, it is a simpler, but non-linear control structure with reduces computational complexity.

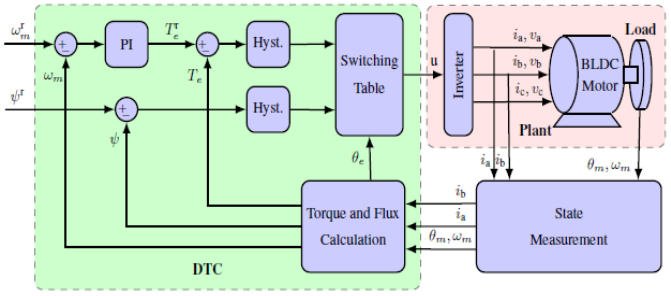

Fig. 4. Block diagram of the BLDC motor control using DTC.

The schematic of DTC is shown in Figure 4. DTC has two control loops, (i) the external speed control and (ii) the internal torque and flux hysteresis loop. Two independent hysteresis controllers produce torque error and stator flux error, and based on those hysteresis controllers' output and stator flux angle, optimum switching logic selects one of the six voltage vectors and two zero voltage vectors from switching table.

C. Hybrid Controller

The principle of the hybrid controller is based on the switching between the two mentioned above techniques. DTC is used in the transient region and FOC in the steady-state region. The transient and steady-state regions are identified by calculating the error (e) between the current speed and the reference value of the speed ($e = \omega_r$ - ω). The control action of the hybrid controller is obtained as follows:

$$u = \begin{cases} DTC, & \text{if } e \le \varepsilon \\ FOC, & \text{otherwise} \end{cases} \quad (12)$$

where ε is the threshold valued of speed error to switch between transient and steady-state regions. Here, we consider ε=0.1.

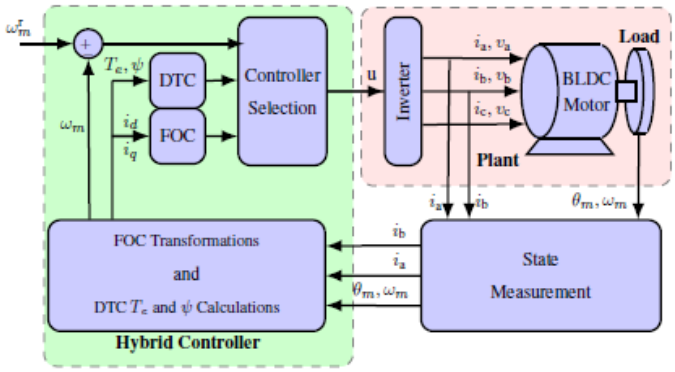

Fig. 5. Block diagram of BLDC motor control using the hybrid technique.

The schematic of the hybrid controller is shown in Figure 5. The controller selection block selects the FOC and DTC with e value, and finally, the control signal, u is applied to the inverter.

D. Non-linear Model Predictive Controller

It is an optimal control method, where the control actions are obtained by solving a Constraint Finite-Time Optimal Control (CFTOC) (see Chapter 1 in [22]).

Figure 6 shows the idea of using centralized NMPC for the speed control of the BLDC motor. The NMPC algorithm is comprised of the nonlinear prediction model, integrator, user-defined constraints, and cost function, and a Non-Linear Programming (NLP) solver to solve the constructed Optimization Control Problem (OCP). We used a zero-order hold sampling for discretization and the Runge Kutta 4th order method for the approximation of the nonlinear function. The NMPC as a direct solution of the CFTOC problem for the reference track is represented as follows:

$$\min_{U} \sum_{k=1}^{N} (\| \omega_{m,k} - \omega_{m,k}^{r} \|_{Q}^{2} + \| \Delta u_k \|_{R}^{2} + \| I_{d,k} \|_{P}^{2}) \quad (13a)$$

Subject to:

$$x_{k+T_s} = f(x_k, u_k), \quad k = 1, \ldots\ldots N \quad (13b)$$

$$\omega_{m,k} = g(x_k, u_k), \quad k = 1, \ldots\ldots N \quad (13c)$$

$$\Delta u_k = u_k - u_{k-1}, \quad k = 1, \ldots\ldots, N \quad (13d)$$

$$-48 \le u_k \le 48, \quad k = 1, \ldots\ldots, N \quad (13e)$$

$$u_{-1} = u(t - T_s), \quad k = 1, \ldots\ldots, N \quad (13f)$$

$$x_0 = x(t), \quad k = 1, \ldots\ldots, N \quad (13g)$$

where, x ϵ R^x, $\omega_{m,k} \epsilon$ R^{ny}, and $u \epsilon R^{nu}$ are the vectors of state, output, and input respectively. ω_m^r is the reference trajectory of speed reference and ω_m is the output or the measured speed. The function f in (13b) describes the nonlinear dynamics of the combined BLDC motor as given by (9), g in (13d) is the speed measurement function.

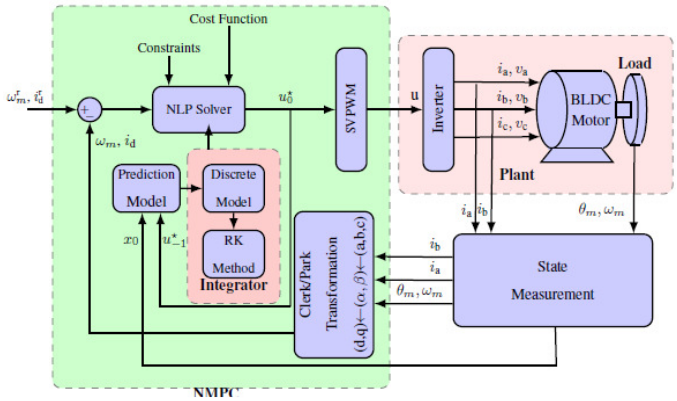

Fig. 6. Block diagram of the BLDC motor control using NMPC.

IV. RESULTS AND DISCUSSION

In this section, the controllers are tested for step-change response and EDC profile. Moreover, we present the numerical analysis of control techniques based on several Key Performance Indices (KPIs) and energy consumption. The current and voltage of phase C are shown as representatives, as all phases are having the same trend with a phase shift of 120°.

A. Speed Torque Characterisitc

Speed torque characteristic gives information about the maximum possible torque delivered by a controller at each speed value. As per (4b), it is the product of BEMF and current, hence different current control techniques produce different torques and different speed-torque characteristics. It must be noted that the torque and speed plotted in the characteristic plot of Figure 7 are measured at the shaft of the motor. Along with controller's characteristics, Figure 7 also contains three reference profiles, which are designed as per the requirements from Table I, named as constant acceleration

(T1), constant energy (P4), and zero acceleration (T3) torque profiles. The T1 torque profile is nothing but the torque required to maintain an acceleration of 2m/s^2 at each speed value, the P4 torque profile indicates the torque at each speed value for constant energy of 3KW, and T3 torque profile indicates the torque required to cruise the vehicle at a constant speed.

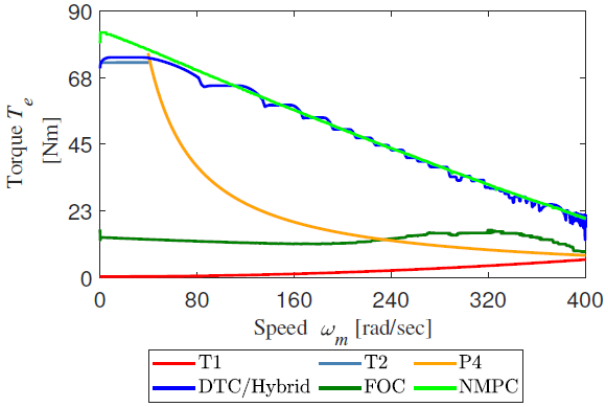

Fig. 7. Controller's speed-torque characteristics against minimum speed-torque characteristics required for the considered EV.

In the case of the hybrid controller, the maximum torque delivered for the respective speed is decided by DTC. Therefore, the torque-speed characteristic curve of DTC and hybrid is the same. If we observe Figure 7 closely, all controllers except FOC are above reference lines T2 and P4. Therefore, DTC, hybrid, and NMPC guarantee the fulfillment of performance specifications. Due to this, FOC delivers less torque than the required and makes it sluggish. Even though FOC does not provide sufficient acceleration, it can maintain the current speed because its generated torque is greater than T3. This is the reason why the hybrid controller switches to FOC in steady-state. To get more insight into the above discussion, we will further analyze the step and EDC speed profile responses.

B. Step Response

All controllers are tested considering the reference step input of 15Kmph and speed, torque, current, and voltage of each one were monitored.

1) Field Oriented Control

Figure 8 shows the performance of the FOC in tracking the desired speed. Figure 8(a) depicts the speed response, Figure 8(b) the generated torque, Figure 8(c) the sinusoidal current excitation required to achieve the desired speed, and Figure 8(d) shows the input voltage applied by the FOC controller. The FOC achieves reference speed after 9.7s. This sluggish response is acquired because the generated torque is smaller than the required value.

2) Direct Torque Control

Figure 9 shows the performance of DTC for step response. The DTC technique tracks the reference speed sooner than FOC at the cost of higher current and torque ripples. Due to the higher current, DTC consumes more energy.

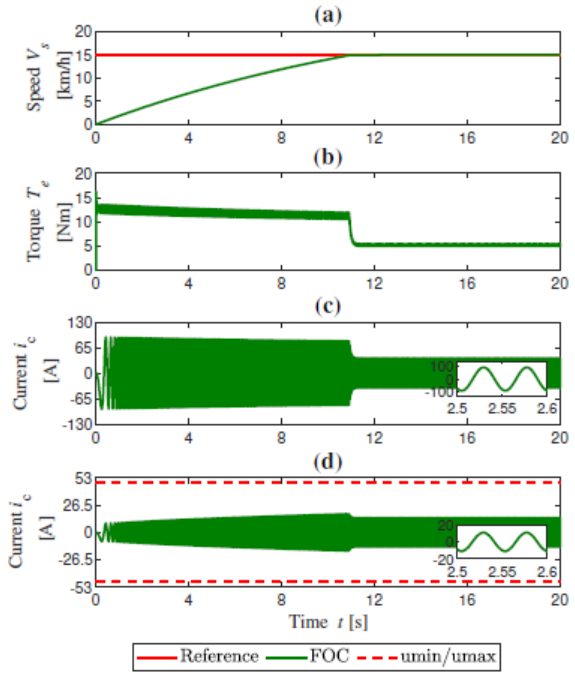

Fig. 8. FOC control with step change in reference input for BLDC motor control with EV load: (a) speed, (b) torque, (c) current, and (d) voltage.

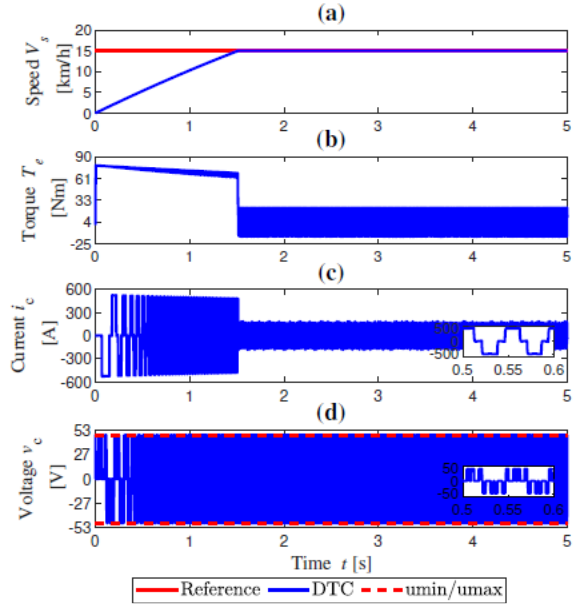

Fig. 9. DTC control with step change in reference input for BLDC motor control with EV load: (a) speed, (b) torque, (c) current, and (d) voltage.

3) Hybrid Control

Figure 10 shows the step response of the hybrid control technique. The hybrid controller exhibits the combined effect of FOC and DTC with fast reference tracking like DTC (Figure 10(a)), reduced torque ripples (Figure 1(b)) due to the FOC, and reduced current and energy consumption due to the FOC (Figure 10(c)). Figure 10(a) also shows the controller selection mode, with zero as DTC during transients' region and 5 for FOC in steady state region.

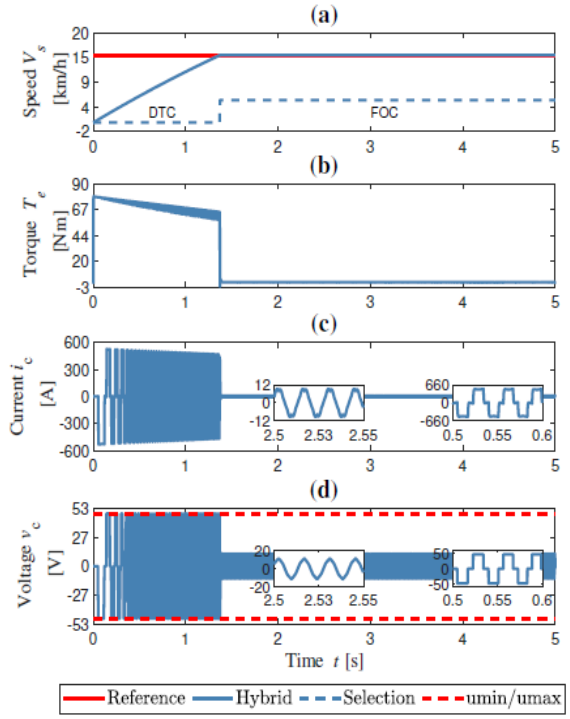

Fig. 10. Hybrid control with step change in reference input for BLDC motor control with EV load: (a) speed, (b) torque, (c) current, and (d) voltage.

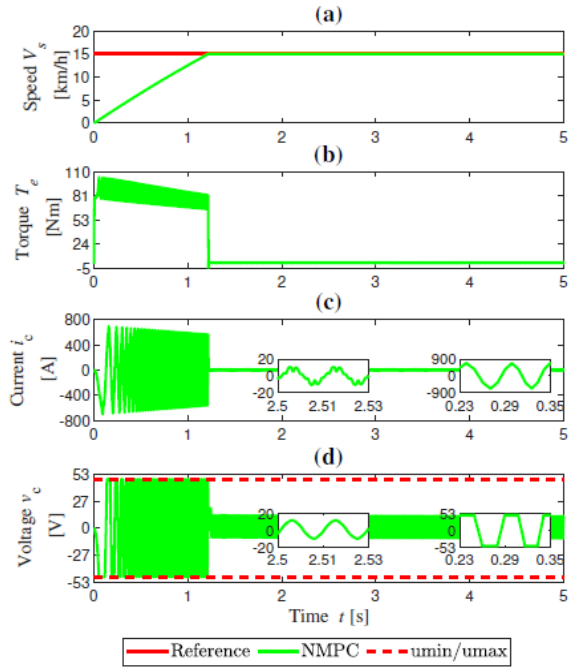

Fig. 11. NMPC control with step change in reference input for BLDC motor control with EV load: (a) speed, (b) torque, (c) current, and (d) voltage.

4) Nonlinear MPC

Figure 11 shows the step response of the NMPC technique. It can be seen that the NMPC achieves the desired speed much faster than other controllers (Figure 11(a)). But this faster response comes at the cost of more torque ripples and higher current and energy consumption during transients (Figure 11(b)-(d)). In steady-state, torque ripples, current, and voltage consumption are comparatively less. One more interesting observation is that as the motors speed approaches the set-point, the ripples are reducing.

TABLE IV. KPIS OF THE CONTROL TECHNIQUES FOR STEP KPIS IN REFERENCE OUTPUT

KPI	FOC	DTC	Hybrid	NMPC
Transient time	11.25	1.41	1.41	1.25
RMSE (%)	100	2.02	12.34	0.10
ME (%)	100	1.55	12.31	0.08
IAE (%)	100	2.01	12.34	0.10
ISE (%)	100	0.04	1.52	0.0001
ISCE (%)	99.82	99.54	100	99.0

5) Result Comparison

Table VI gives the summary of all the KPIs for the controllers and their performance regarding step response. From Table VI, it can be seen that the NMPC technique outperforms the other techniques, because the other techniques (DTC, FOC, and hybrid) are based on a fixed or finite combination of current excitation, whereas NMPC does optimal modulation in the current excitation. This optimal modulation in the current reflects on the Total Harmonic Distortion (THD) of the in-phase current. In the trapezoidal control (DTC), the THD is around 8%, in FOC it is 3% and for NMPC, as the optimal excitation varies, the THD varies between 4% and 7%. These ripples are required by considering the non-sinusoidal BEMF of the motor. In case of a sudden change in the set-point, the controller has to drive the motor with maximum torque, so NMPC tries to deliver maximum current without much caring about torque ripples, but as the motor approaches the set-point, the current approaches the minimum value with minimum ripples in current and torque.

C. Ramp Response

The hybrid controller selects either FOC or DTC based on the error threshold, but during the ramp type speed reference, if the controller selects the DTC, then the response cannot be energy efficient and if FOC is selected, then the controller cannot track the reference speed. In this view, a hybrid controller either toggles the two sub-controllers or selects only DTC without much caring about energy efficiency. This problem occurs only in the case of the hybrid controller. Therefore, in this section, this problem is addressed and the outcome is compared with NMPC.

1) Hybrid

To get efficient operation if the controller follows the toggling case, the results will be as shown in Figure 12. Due to the continuous switching between DTC and FOC there are ripples in speed and eventually this is reflected on voltage and current. This frequent switching can be avoided by using a hysteresis controller for DTC/FOC selection, but this controller will be either overexcited (DTC) or sluggish (FOC).

2) NMPC

Figure 13 depicts the NMPC response for ramp type speed reference. The NMPC shows better tracking with minimum error. This is due to the modulation in current excitation as per

the operating conditions. This modulation in current excitation helps making a smooth transition from transient region to steady-state region, with the desired performance.

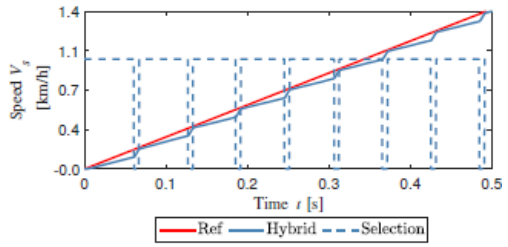

Fig. 12. Enhanced view of motor speed tracking in ramp type reference.

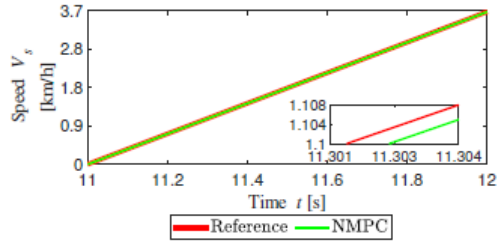

Fig. 13. Ramp response of the NMPC for speed control of a BLDC driven EV.

D. European Driving Cycle

The hybrid controller combines the advantages of DTC and FOC. Therefore, in this section, we test the performance of hybrid control and NMPC techniques in real-life scenarios, which can be tested through the EDC. Both the controllers are tested for speed tracking as per torque given through EDC. Figure 14 depicts the response of both techniques. Figure 14(a) shows the speed and Figure 14(b) shows the desired and achieved torque. It can be seen that both controllers perform well regarding the tracking of the desired speed. However, the hybrid controller shows higher torque ripples and over-excitation of the motor with high oscillation in the current due to the higher voltage input during the DTC selection. As a consequence, the hybrid controller consumes more energy. Similar inference is generated by the different KPI's in Table V.

TABLE V. KPIS OF THE CONTROL TECHNIQUES FOR EDC

KPI	FOC	DTC	Hybrid	NMPC
RMSE (%)	100	4.38	0.29	0.02
ME (%)	100	3.46	0.29	0.026
IAE (%)	100	5.43	0.74	0.022
ISE (%)	100	0.192	0.025	0.0001
ISCE (%)	99.001	100	99.019	99.008
Energy (%)	53	100	50	47

According to Table V, FOC does not perform well. It shows higher RMSE and generates less torque. FOC can't compete, even in minimum energy consumption. Also, it is worth noting that the hybrid controller shows better RMSE and IAE, but consumes more energy. Overall, the proposed NMPC controller works smoothly and outperforms the other techniques. In summary, the drawbacks of the DTC and FOC techniques are removed by the hybrid controller by selecting DTC and FOC as per requirements based on the speed error value. However, due to the sudden switching between DTC and FOC, a smooth transition is not possible for variable reference. This smooth transition requires an optimum modulation of excitation current waveform, which can produce the best solution to avoid over-excitation and torque ripples, and this has been achieved with the NMPC controller.

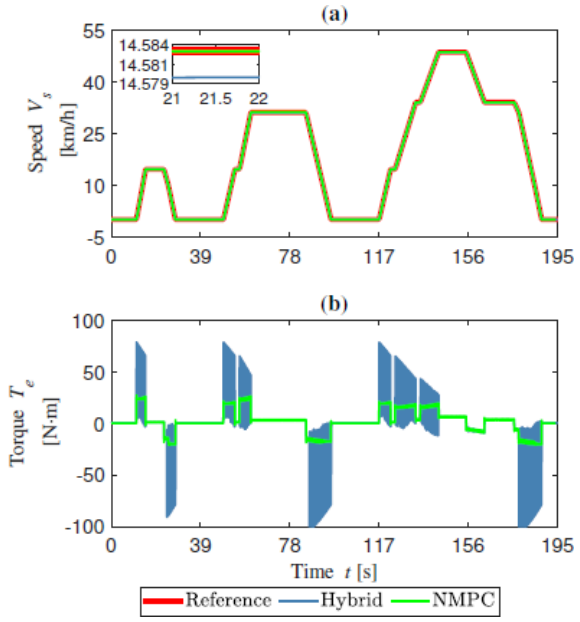

Fig. 14. Hybrid and NMPC controllers response over the european driving cycle profile: (a) speed and (b) torque.

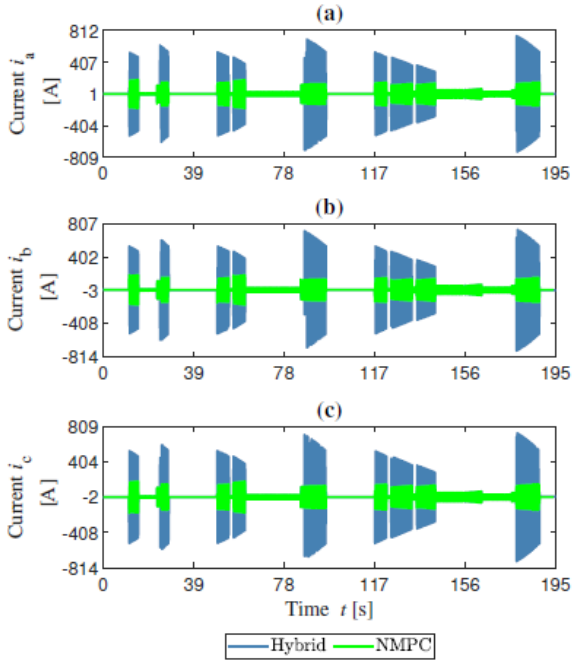

Fig. 15. Current response of hybrid and NMPC controllers over the EDC profile: (a) phase A, (b) phase B, and (c) phase C.

V. IMPLEMENTATION ASPECTS

In real life, we need to implement motor control techniques on portable and resource-limited hardware like microcontrollers and/or FPGA. Below, we will discuss the implementation aspects of the NMPC technique.

- Prediction model: the success of NMPC depends on the accuracy of the system model. Therefore, it is important to have an accurate model of the motor to capture nonlinear dynamic behavior.
- Embedded implementation: In recent years, there have been several works on the embedded implementation of NMPC solvers, which allow deploying the whole algorithm on embedded devices [22, 24].
- Controller complexity: Due to the optimization, NMPC is a complex controller, and its complexity increases with the problem size (number of states, inputs, constraints, and prediction horizon). Several approaches have been presented to design low-complexity NMPC [22, 24].
- State and disturbance estimation: As an NMPC is a state-feedback control technique, it is important to obtain accurate values of the states. Furthermore, estimation methods can be used to estimate model parameters.

VI. CONCLUSION

In this paper, we showed the applicability of a nonlinear MPC to control the BLDC motor for a three-wheeler EV. The proposed NMPC technique improves the closed-loop control performance, reduces energy consumption and steady-state errors. The NMPC is designed with a nonlinear model of the BLDC motor with an electric three-wheeler load to obtain the optimal voltage for the regulation of motor torque. Another significant contribution of this paper is the performance assessment of the four considered control techniques. The proposed NMPC shows smooth operation and gives optimal control actions in the transients and steady-state regions. Therefore, in our assessment, it is concluded that the designed NMPC is best suited for the electric three-wheeler application, where abruptly changing set-points generates more transients. The future goal of this work is to implement the proposed NMPC-based control solution on embedded hardware and study its performance on the EV platform.

ACKNOWLEDGMENT

We gratefully acknowledge the Prime Minister's Fellowship for Doctoral Research, the TEQIP project of COEP, and HELLA Automotive India Pvt. Ltd.

REFERENCES

[1] G. Gururaj and K. S. Gowri, "Performance Optimization of an eCAR by Parametric Analysis," *Engineering, Technology & Applied Science Research*, vol. 9, no. 6, pp. 4968–4973, Dec. 2019, https://doi.org/10.48084/etasr.3139.

[2] D. B. Minh, V. D. Quoc, and P. N. Huy, "Efficiency Improvement of Permanent Magnet BLDC Motors for Electric Vehicles," *Engineering, Technology & Applied Science Research*, vol. 11, no. 5, pp. 7615–7618, Oct. 2021, https://doi.org/10.48084/etasr.4367.

[3] M. Garcia, P. Ponce, L. A. Soriano, A. Molina, B. MacCleery, and D. Romero, "Lifetime Improved in Power Electronics for BLDC Drives using Fuzzy Logic and PSO," *IFAC-PapersOnLine*, vol. 52, no. 13, pp. 2372–2377, Jan. 2019, https://doi.org/10.1016/j.ifacol.2019.11.561.

[4] K. D. Carey, N. Zimmerman, and C. Ababei, "Hybrid field oriented and direct torque control for sensorless BLDC motors used in aerial drones," *IET Power Electronics*, vol. 12, no. 3, pp. 438–449, 2019, https://doi.org/10.1049/iet-pel.2018.5231.

[5] K. S. Belkhir, "Simple Implementation of a Fuzzy Logic Speed Controller for a PMDC Motor with a Low Cost Arduino Mega," *Engineering, Technology & Applied Science Research*, vol. 10, no. 2, pp. 5419–5422, Apr. 2020, https://doi.org/10.48084/etasr.3340.

[6] N. H. Mugheri and M. U. Keerio, "An Optimal Fuzzy Logic-based PI Controller for the Speed Control of an Induction Motor using the V/F Method," *Engineering, Technology & Applied Science Research*, vol. 11, no. 4, pp. 7399–7404, Aug. 2021, https://doi.org/10.48084/etasr.4255.

[7] P. Vas, *Vector Control of AC Machines*. Oxford, UK: Clarendon Press, 1990.

[8] J. P. John, S. S. Kumar, and B. Jaya, "Space Vector Modulation based Field Oriented Control scheme for Brushless DC motors," in *International Conference on Emerging Trends in Electrical and Computer Technology*, Nagercoil, India, Mar. 2011, pp. 346–351, https://doi.org/10.1109/ICETECT.2011.5760141.

[9] M. Lazor and M. Stulrajter, "Modified field oriented control for smooth torque operation of a BLDC motor," in *ELEKTRO*, Rajecke Teplice, Slovakia, Dec. 2014, pp. 180–185, https://doi.org/10.1109/ELEKTRO.2014.6847897.

[10] J. Chen, M. Li, and J. Liu, "A new SVPWM-based control scheme of permanent magnetic brushless DC machine with trapezoidal back EMF waveforms," in *33rd Youth Academic Annual Conference of Chinese Association of Automation*, Nanjing, China, Dec. 2018, pp. 1147–1151, https://doi.org/10.1109/YAC.2018.8406544.

[11] S. J. Park, H. W. Park, M. H. Lee, and F. Harashima, "A new approach for minimum-torque-ripple maximum-efficiency control of BLDC motor," *IEEE Transactions on Industrial Electronics*, vol. 47, no. 1, pp. 109–114, Oct. 2000, https://doi.org/10.1109/41.824132.

[12] A. G. de Castro, W. C. A. Pereira, T. E. P. de Almeida, C. M. R. de Oliveira, J. Roberto Boffino de Almeida Monteiro, and A. A. de Oliveira, "Improved Finite Control-Set Model-Based Direct Power Control of BLDC Motor With Reduced Torque Ripple," *IEEE Transactions on Industry Applications*, vol. 54, no. 5, pp. 4476–4484, Sep. 2018, https://doi.org/10.1109/TIA.2018.2835394.

[13] S.-J. Kang and S.-K. Sul, "Direct torque control of brushless DC motor with nonideal trapezoidal back EMF," *IEEE Transactions on Power Electronics*, vol. 10, no. 6, pp. 796–802, Aug. 1995, https://doi.org/10.1109/63.471301.

[14] Y. Liu, Z. Q. Zhu, and D. Howe, "Direct torque control of brushless DC drives with reduced torque ripple," *IEEE Transactions on Industry Applications*, vol. 41, no. 2, pp. 599–608, Mar. 2005, https://doi.org/10.1109/TIA.2005.844853.

[15] H. Aygun and M. Aktas, "A Novel DTC Method with Efficiency Improvement of IM for EV Applications," *Engineering, Technology & Applied Science Research*, vol. 8, no. 5, pp. 3456–3462, Oct. 2018, https://doi.org/10.48084/etasr.2312.

[16] A. Tashakori Abkenar and M. Motamed Ektesabi, "Direct Torque Control of In-Wheel BLDC Motor Used in Electric Vehicle," in *IAENG Transactions on Engineering Technologies*, G.-C. Yang, S. Ao, and L. Gelman, Eds. New York, NY, USA: Springer, 2013, pp. 273–286.

[17] K.-S. Low, K.-Y. Chiun, and K.-V. Ling, "Evaluating generalized predictive control for a brushless DC drive," *IEEE Transactions on Power Electronics*, vol. 13, no. 6, pp. 1191–1198, Aug. 1998, https://doi.org/10.1109/63.728346.

[18] K.-S. Low and H. Zhuang, "Robust model predictive control and observer for direct drive applications," *IEEE Transactions on Power Electronics*, vol. 15, no. 6, pp. 1018–1028, Aug. 2000, https://doi.org/10.1109/63.892816.

[19] J. A. E. Andersson, J. Gillis, G. Horn, J. B. Rawlings, and M. Diehl, "CasADi: a software framework for nonlinear optimization and optimal

control," *Mathematical Programming Computation*, vol. 11, no. 1, pp. 1–36, Mar. 2019, https://doi.org/10.1007/s12532-018-0139-4.

[20] J. Larminie and J. Lowry, *Electric Vehicle Technology Explained*. New York, NY, USA: John Wiley & Sons, 2012.

[21] P. Ubare, D. Ingole, and D. Sonawane, "Energy-efficient Nonlinear Model Predictive Control of BLDC Motor in Electric Vehicles," in *Sixth Indian Control Conference*, Hyderabad, India, Dec. 2019, pp. 194–199, https://doi.org/10.1109/ICC47138.2019.9123204.

[22] L. Grune and J. Pannek, *Nonlinear Model Predictive Control: Theory and Algorithms*. New York, NY, USA: Springer, 2017.

[23] S. Adhau, S. Patil, D. Ingole, and D. Sonawane, "Implementation and Analysis of Nonlinear Model Predictive Controller on Embedded Systems for Real-Time Applications," in *18th European Control Conference*, Naples, Italy, Jun. 2019, pp. 3359–3364, https://doi.org/10.23919/ECC.2019.8796118.

[24] V. Patne, D. Ingole, and D. Sonawane, "FPGA Implementation Framework for Low Latency Nonlinear Model Predictive Control," *IFAC-PapersOnLine*, vol. 53, no. 2, pp. 7020–7025, Jan. 2020, https://doi.org/10.1016/j.ifacol.2020.12.443.